Title

Detection of polymeric silicate in the pore water of freshwater lakes

Author(s)

Ja Yeong Park, Masahito Sugiyama, Shogo Sugahara, Yasushi Seike

1   **Detection of polymeric silicate in the pore water of freshwater lakes**

2

3   **Ja Yeong Park[1,2,*], Masahito Sugiyama[1], Shogo Sugahara[2], Yasushi Seike[3]**

4   [1]Graduate School of Human and Environmental Studies, Kyoto University, Yoshida-

5   Nihonmatsu-cho, Sakyo-ku, Kyoto, 606-8501, Japan

6   [2,*] Interdisciplinary Graduate School of Science and Engineering, Shimane University,

7   1060 Nishikawatsu-cho, Matsue, Shimane, 690-8504, Japan

8   [3]Estuary Research Center, Shimane University, 1060 Nishikawatsu-cho, Matsue,

9   Shimane 690-8504, Japan

10

11   Email address. Ja Yeong Park; park.jayeong.53v@riko.shimane-u.ac.jp

12   Masahito Sugiyama; sugiyama.masahito.5s@kyoto-u.ac.jp

13   Shogo Sugahara; suga@riko.shimane-u.ac.jp

14   Yasushi Seike; yseike@riko.shimane-u.ac.jp

15

16

17   Keywords: polymeric silicate, adsorption, ferric hydroxide, pore water, anoxic-reducing

18   environment

19 **Abstract**

20 Understanding the formation mechanisms of polymeric silicates is essential to the study

21 of microbiology and biogeochemistry. It has implications for the growth of diatoms and

22 dinoflagellates and studying the processes that control the dissolution, precipitation, and

23 biological uptake of different silicates species can provide an understanding of the

24 occurrence of toxic blooms. This study examines the seasonal distribution of

25 monomeric and polymeric silicates in the brackish and freshwater lakes of Japan.

26 Inductively coupled plasma atomic emission spectroscopy was used to detect and

27 quantify total dissolved silicates (TSi) and the spectrophotometric molybdenum blue

28 method was used to detect molybdate reactive silicates (monomers to tetramers). The

29 difference between the concentrations obtained via these two methods was used to

30 determine the concentrations of polymeric silicates. Polymeric silicates were detected in

31 anoxic-reducing pore waters from sediments of the freshwater Lake Biwa and Lake

32 Kawaguchi in Japan, with a maximum concentration of 0.42 mmol L^{-1}. Polymeric

33 silicate was continuously detected as long as the lake bottom environments remained

34 under anoxic-reducing conditions. It provides insights on the formation mechanisms of

35 polymeric silicates in freshwater lakes. The polymerization of silicates is understood to

36 occur during the adsorption reaction between monomeric silicates and $Fe(OH)_3$

37 precipitate. Furthermore, this polymerization is deemed to be a dehydration

38 condensation reaction because the silicates adsorbed on $Fe(OH)_3$ precipitate are situated

39 at short distances from each other. In the anoxic-reducing environments, these

40 monomeric and polymeric silicates are released from ferric hydroxide $(Fe(OH)_3)$

41 precipitate by reacting with hydrogen sulfide.

Introduction

Dissolved silicate is an essential nutrient for aquatic organisms, and it is mainly used by diatoms to form their skeletons (Perry and Keeling-Tucker 2000; Yee et al. 2003; Lacombe et al. 2007). Diatoms account for approximately 25% of the global net primary production of aquatic organisms (Willén 1991) and interfere with the growth of dinoflagellates which are among the leading causes of red tides (Furumai 2012).

Dissolved silicate is supplied to lakes and oceans through rivers and groundwater (Ning 2002; Lacombe et al. 2007; Cornelis et al. 2011). Soluble silicate is usually in the form of a monomer (H_4SiO_4). The average concentrations of dissolved silicate are 0.2 mmol L^{-1} in freshwaters (Aston 1983; Willén 1991) and 0.1 mmol L^{-1} in oceans (Tréguer et al. 1995).

Dissolved silicate is removed from the water column via two pathways: biological uptake, such as that which occurs during excessive growth of diatoms (Schelske and Stoermer 1971; Li et al. 2006); and precipitation, caused by the adsorption of dissolved silicate onto $Fe(OH)_3$ precipitate (Tallberg 2000). These precipitates sink to the bottoms of lakes and oceans and are buried in the sediment for long periods, as long as the environment remains oxidative. Eventually, the dissolved silicate in a lake becomes depleted (Fischer and Knoll 2009).

When the concentration of dissolved monomeric silicate exceeds 1.4 mmol L^{-1} in 15 °C water, the silicates are converted to various polymeric silicate species (Zuhl and Amjad 2013). Some researchers have mentioned the presence of polymeric silicate species in natural waters with low molecular weights, ranging from silicate dimers to pentamers, at concentrations below their solubilities (George et al. 2000; Tanaka et al. 2013). These silicate species can be measured using the molybdenum blue method

66   (O'Connor 1961).

67   Diatoms can biologically utilize dissolved silicates ranging from monomers to linear

68   tetramers (Tanaka et al. 2013). The growth of diatoms is depressed by a lack of these

69   light silicates and an increase in polymeric silicates with high molecular weights. A lack

70   of diatom growth results in the rapid growth of harmful phytoplankton (Schelske and

71   Stoermer 1971; Conley et al. 1993), such as dinoflagellates that produce neurotoxins

72   (Wang 2008). Therefore, a study on the formation mechanisms of polymeric silicates is

73   essential from the perspectives of microbiology and biogeochemistry.

74   Gas-liquid chromatography (Tarutani 1989) and nuclear magnetic resonance spectra

75   (Sjöberg 1996) are applied as qualitative and quantitative methods for analyzing

76   polymeric silicates. However, the most convenient analytical method is to combine

77   inductively coupled plasma atomic emission spectroscopy (ICP-AES) and the

78   spectrophotometric molybdenum blue method. According to O'Connor (1961),

79   dissolved silicates that are monomers to linear pentamers are measurable within 5 min

80   of the reaction time using the molybdenum blue method. The ICP-AES can measure TSi

81   irrespective of the chemical species in the solutions (Tallberg 2000). Therefore, the

82   concentration of polymeric silicates larger than pentamers can be calculated as the

83   difference between the analytical results of ICP-AES and those of the molybdenum blue

84   method.

85   Isshiki et al. (1991) analyzed seawater using this method and reported that the

86   concentration of TSi increased with water depth; however, they could not observe a

87   difference between ICP-AES results and those of the molybdenum blue method. They,

88   therefore, concluded that polymeric silicate did not exist in seawater.

89   However, polymeric silicates have been found to occur seasonally in the pore water

4

90   of freshwater lakes such as Lakes Biwa and Kawaguchi in Japan (Park and Sugiyama

91   2018). Although the TSi concentrations were lower than the solubility of monomeric

92   silicate, polymeric silicates were detected in the pore water. In contrast, polymeric

93   silicates were not detected in brackish lake waters since the analytical results of ICP-

94   AES and the molybdenum blue method were precisely the same for all brackish lakes

95   such as Lakes Nakaumi, Suigetsu, and Suga in Japan. In freshwater lakes, the lake

96   bottom environment changes to an anoxic-reducing environment during summer,

97   causing a rapid increase in the concentrations of TSi and $H_2S + HS^-$ in the pore water.

98   This phenomenon indicates that the elution mechanism of silicates in freshwater lakes

99   may be similar to that of phosphates in anoxic-reducing environments (Valdes et al.

100   2002). Although Swedlund and Webster (1999) reported that the eluted silicate was

101   adsorbed onto the surface of $Fe(OH)_3$ to form a polymer, there has been no report on the

102   chemical species of dissolved silicates in anoxic-reducing lake sediments. Furthermore,

103   the adsorption and desorption processes of dissolved silicates and the stability of

104   polymeric silicates remain poorly understood. In this study, we discuss the seasonal and

105   vertical distributions of monomeric and polymeric silicates in the sediment of some

106   brackish and freshwater lakes of Japan and clarify the formation mechanism of

107   polymeric silicate by investigating polymerization sites and timing that occurs during

108   the adsorption reaction between dissolved silicates and $Fe(OH)_3$.

109

110

111   **Materials and methods**

112   **Study areas**

113   As the representative of brackish lakes, we selected Lakes Nakaumi, Suigetsu, and

114   Suga in Japan. These lakes have sufficiently abundant dissolved salts to classify them as

115   brackish lakes. The salinities in the hypolimnion layers are all above 10 psu (g kg^{-1}), at

116   30, 12, and 11 psu for Lakes Nakaumi, Suigetsu, and Suga, respectively.

117   Previous studies have reported that these lakes are eutrophic (Maekawa et al. 1982;

118   Kusunoki and Sakata 2018). We observed that anoxic and reducing conditions were

119   reinforced during the summer season at the sampling points, located at 35.43°N,

120   144.27°E in Lake Nakaumi, 35.58°N, 135.88°E in Lake Suigetsu, and 35.58°N,

121   135.90°E in Lake Suga (Fig. 1). The water depths at the sampling points in Lakes

122   Nakumi, Suigetsu, and Suga were 15, 33, and 12 m, respectively.

123   As the representative of freshwater lakes, we selected Lakes Biwa and Kawaguchi in

124   Japan. Lake Biwa is the largest lake in Japan. It is situated in the western part of Japan

125   (Fig. 1, 35.52°N, 136.20°E; Tanaka 1992) and can be divided into the northern and

126   southern basins (Pollingher 1990). The southern basin is eutrophic and has an average

127   depth of 5 m, with algal blooms occurring periodically in summer (Nalewajko and

128   Murphy 2001). In this study, water and sediment samples were collected from February

129   to December 2017 from an area (Fig. 1, 35.00°N, 135.57°E), in the south-eastern part of

130   the southern basin, which was dredged to provide sediments and soils for the

131   construction of an artificial island alongside it (Terashima and Ueda 1982). The samples

132   were collected from a maximum depth of 13 m below the surface of the lake over an

133   area of 0.25 km^2. An anoxic hypolimnion typically appears in this area for several

134   months of the year due to the thermal stratification of lake water during summer

135   (Kawashima et al. 1985).

136   Lake Kawaguchi is located in the central part of Japan (Kyotani et al. 2005;

137   Yamamoto et al. 2017). This lake is eutrophic, can be divided into the western, eastern,

138 and Funatsu (south-eastern) basins and has a maximum water depth of 16.1 m

139 (Nagasaka et al. 2002). Samples were collected at 35.51°N, 138.73°E from a depth of

140 11.3 m in the western basin (Fig. 1), where dissolved oxygen typically undergoes

141 seasonal depletion in the hypolimnion layer, similar to the dredged area of Lake Biwa.

142

143 **Sampling and pretreatment**

144 Water depth, electrical conductivity, water temperature, dissolved oxygen (DO), and

145 chlorophyll-a were measured using a multi water-quality profiler (Rinko-Profiler ASTD

146 102, JFE Advantech Co., Ltd., Japan). All water samples were collected using a water

147 sampler (Niskin-X sampling bottles, General Oceanics, Inc., USA) and filtered using

148 0.45-μm polyvinylidene difluoride (PVDF) filters (Millex-HV syringe filter, Merck

149 Millipore Ltd., Germany) within 2 h of collection. Ultrapure nitric acid (HNO_3, 60 %,

150 Kanto Kagaku, Japan) was added to all filtrates to adjust the concentration of HNO_3 to

151 0.02 mol L^{-1} and prevent the formation of $Fe(OH)_3$.

152 Sediment samples were collected using a core sampler (HR-type core sampler, Rigo,

153 Co., Inc., Japan). Pore water samples were filtered through a 0.45-μm PVDF filter, and

154 HNO_3 was added to the filtrate as described above.

155

156 **Reagents**

157 Highly purified Milli-Q water (Milli-Q Water Purification System ZD21-100sp,

158 Millipore, Japan) was used in all laboratory experiments. Deoxygenated water was

159 prepared by bubbling 99.99% nitrogen gas into 1000 mL of Milli-Q water for 1 h before

160 use. In laboratory experiments, the pH of each sample solution was adjusted to 7 using

161 dilute HCl or NaOH solutions.

162 Silicon standard solution (1000 mg-Si L^{-1}, Na_2SiO_3 in 0.2 mol L^{-1} Na_2CO_3, Wako

163 Pure Chemical Industries, Ltd., Osaka, Japan) was used to analyze silicates. Moreover,

164 disodium molybdate (VI) dihydrate ($Na_2MoO_4 \cdot 2H_2O$, Wako Pure Chemical Industries,

165 Ltd., Osaka, Japan) was used as a coloring reagent. L-(+)-tartaric acid (Nakarai Tesque,

166 INC., Kyoto, Japan) was used to remove the interference of phosphate. L-(+)-ascorbic

167 acid (Wako Pure Chemical Industries, Ltd., Osaka, Japan) was used as a reducing agent

168 for yellow silico-molybdate complexes.

169 The dissolved iron (DFe; Fe^{3+}) solution was prepared using an iron standard solution

170 (1000 mg-Fe L^{-1}, $Fe(NO_3)_3$ in 0.275 mol L^{-1} HNO_3 (Nakarai Tesque, INC., Kyoto,

171 Japan)). The Na_2S solution was prepared by dissolving sodium sulfide nonahydrate

172 ($Na_2S \cdot 9H_2O$, Wako Pure Chemical Industries, Ltd., Osaka, Japan) in deoxygenated

173 Milli-Q water, prepared as mentioned above.

174

175 **Determination of dissolved silicate, dissolved iron, and total dissolved hydrogen**

176 **sulfide**

177 A spectrophotometer (Autoanalyzer, UV-VIS Spectrophotometer II, Bran Luebbe,

178 Japan) and an inductively coupled plasma atomic emission spectrometer (ICP-AES;

179 Optima 5000Z, Perkin-Elmer, Japan) were used to measure the concentration of

180 dissolved silicate and distinguish the silicate species. Spectrophotometric determination

181 of dissolved silicate was carried out using the molybdenum blue method at 660 nm

182 (Hansen and Koroleff 1999).

183 In this study, the dissolved silicate concentrations measured using a

184 spectrophotometer and ICP-AES are expressed as molybdate reactive silicates (MSi:

185 silicates ranging from monomer to linear pentamer species (O'Connor 1961)) and TSi,

186   respectively. The concentration of dissolved polymeric silicates (PSi: polymerized

187   silicate species larger than pentamers) was calculated by subtracting MSi concentrations

188   from TSi concentrations.

189   Dissolved iron and total hydrogen sulfide concentrations were analyzed using ICP-

190   AES and spectrophotometry, respectively. Spectrophotometric determination of total

191   hydrogen sulfide was carried out using the methylene blue method at 667 nm (Sugahara

192   et al. 2010).

193

194   **Laboratory experiments**

195   **Adsorption of dissolved silicate onto ferric hydroxide**

196   In the adsorption reaction of dissolved silicates onto $Fe(OH)_3$, the polymerization

197   ratio of silicates was examined for 120 days. A mixed solution was prepared, containing

198   0.7 mmol L^{-1} of MSi and 0.1 mmol L^{-1} of DFe. To confirm the polymeric silicate

199   production by adsorption, the molar concentration ratio of Si: Fe in the mixed solution

200   was set to 7:1. The pH value of this solution was adjusted to 7.0 using the minimum

201   required volume of concentrated NaOH or HCl solutions to form $Fe(OH)_3$ precipitates.

202   This solution was stored for 120 days at ambient temperature.

203   A 10 mL quantity of the mixed solution was collected on particular days, and then

204   immediately filtered using a Nucleopore filter (pore size: 0.40 μm, diameter: 47 mm,

205   Whatman). The MSi and TSi in the filtrate were then measured. The precipitate

206   collected on the filter was reacted with 10 mL of 0.02 mol L^{-1} HNO_3 solution for one

207   day until it dissolved into the solution. The MSi and TSi concentrations in this solution

208   were measured. PSi concentrations were calculated from these MSi and TSi

209   concentrations.

210

Stability of PSi

212   The experiments were performed in the order shown in Fig. 2. The $Fe(OH)_3$ was

213   precipitated in a mixed solution (1.0 mmol L^{-1} of MSi, 0.1 mmol L^{-1} of DFe) by

214   adjusting the pH of the solution to 7.0. After 6 months, this solution was divided into

215   four fractions. Each fraction was then filtered through 0.40-μm Nucleopore filters. The

216   MSi and TSi concentrations in each filtrate were measured using the molybdenum blue

217   method and ICP-AES, respectively.

218   The precipitates were treated using the procedure shown in Fig. 2. To quantify the

219   relative proportions of MSi and PSi under oxic and anoxic conditions, we divided the

220   experimental conditions into four fractions, such as HNO_3 + Aeration, HNO_3 +

221   Anaeration, Na_2S + Aeration, and Na_2S + Anaeration.

222   The precipitate of the first fraction was added to 100 mL of 0.02 mol L^{-1} HNO_3 (pH

223   2.20 ± 0.03) to dissolve the $Fe(OH)_3$ precipitate. Prior to this procedure, the HNO_3

224   solution was well aerated by bubbling atmospheric air filtered with air filters (CCF-050-

225   D1B and CCF-010-D1B, Capsule filter, pore size: 0.5 and 0.1 μm, Advantec, Japan),

226   and the DO concentration was approximately 8.9 mg-O_2 L^{-1}. This solution was re-

227   filtered with a Nucleopore filter (pore size: 0.20 μm, diameter: 25 mm, Whatman). This

228   re-filtrate was continuously monitored for changes in the concentrations of MSi, PSi,

229   TSi, DO, and total dissolved hydrogen sulfide (H_2S + HS^-) for 14 days under ambient

230   air conditions and room temperature. This experimental condition is hereafter referred

231   to as "HNO_3 + Aeration".

232   The second fraction was also dissolved with 100 mL of 0.02 mol L^{-1} HNO_3 (pH 2.20

233   ± 0.03). However, this HNO_3 solution was first deoxygenated by bubbling with nitrogen

234   gas. This solution was also re-filtered and then stored in a polyethylene bottle sealed

235   with plastic film. This bottle was put into a polyethylene bag together with an open

236   bottle containing Na_2SO_3 solution, as an oxygen-adsorbing agent, to protect from the

237   invasion of atmospheric oxygen. This experimental condition is hereafter referred to as

238   "HNO_3 + Anaeration". The filtrate was continuously monitored in a manner similar to

239   that for the first fraction.

240   The precipitates from the third and fourth fractions were reacted with 100 mL of 0.3

241   mmol L^{-1} Na_2S solution (pH 7.10 ± 0.05) for one day. The $Fe(OH)_3$ precipitate was

242   converted to ferrous sulfide precipitate. Here, the Na_2S solution was prepared using

243   deoxygenated Mili-Q water. Each solution was filtered again using a 0.20-µm

244   Nucleopore filter to obtain the re-filtrate. These solutions were stored under aerobic and

245   anaerobic conditions for 14 days, respectively. They were also continuously monitored,

246   as in the case of the first fraction. These experimental conditions are hereafter referred

247   to as "Na_2S + Aeration" and "Na_2S + Anaeration", respectively.

248

249

250   **Results and Discussion**

251   **Distribution of silicate species in brackish lakes**

252   Figures 3 and 4 show MSi and TSi concentrations in the pore waters of each

253   brackish lake. In Lakes Nakaumi, Suigetsu, and Suga, MSi concentrations coincided

254   with TSi concentrations in the pore waters. However, we noted the absence of PSi in the

255   brackish lakes, even though the TSi concentration in the pore water of Lake Nakaumi

256   was five times the solubility of MSi. In pore water of brackish lakes, the concentration

257   of dissolved silicates exceeded by the solubility of MSi is attributed to the reduction of

11

258   Fe(OH)$_3$ by H$_2$S in the anoxic-reducing environment; the subsequent reactions result in

259   the formation of ferrous sulfide (FeS) and the dissolution of silicates that had been

260   adsorbed onto Fe(OH)$_3$. The same situation has been reported for Lake Nakaumi in our

261   previous work (Park et al. 2020). Even from a thermodynamic point of view, this

262   hypothesis is sufficiently valid. Fukusawa et al. (1995) have already shown that the iron

263   in a brackish lake such as Lake Suigetsu is directly reduced by H$_2$S. They suggest that

264   the iron reduction process depends on the lake water characteristics. Furthermore,

265   Lehtoranta et al. (2009) reported that the eutrophication of lakes had accelerated the

266   conversion of the dominant species from iron-reducing bacteria to sulfate-reducing

267   bacteria. This change in the biogeochemical characteristics of the sediments accelerates

268   the production of H$_2$S, which then directly reduces Fe(OH)$_3$.

269

270   **Distribution of silicate species in freshwater lakes**

271   Figure 5 shows the vertical distribution of DO in the water columns of Lakes Biwa

272   (September 21, 2017) and Kawaguchi (September 30, 2017). Figures 6 and 7 show the

273   vertical distributions of DFe, H$_2$S + HS$^-$, TSi, MSi, and PSi concentrations in pore

274   waters of the freshwater lakes. In both lakes, the DO was depleted in the pore water and

275   hypolimnion layer (Fig. 5). The TSi concentration in the pore water was slightly higher

276   in Lake Biwa than in Lake Kawaguchi, but the difference was not significant. The PSi

277   concentrations were 0 to 0.42 mmol L^{-1} in Lake Biwa and 0 to 0.23 mmol L^{-1} in Lake

278   Kawaguchi (Fig. 7). The concentrations of DFe and H$_2$S + HS$^-$ in the pore waters were

279   higher in Lake Biwa compared to that in Lake Kawaguchi (Fig. 6).

280   Figure 8 shows the variation of DO concentration at a depth of 12 m (just above the

281   lake bottom) in Lake Biwa from February 14 to December 15, 2017. From February to

282   April and from October to December, the DO was high in the hypolimnion layer.

283   However, from mid-May to mid-September, the environment of the bottom layer was

284   anoxic and reducing (Fig. 8), and concentrations of DFe, $H_2S + HS^-$, and TSi increased

285   (Fig. 9). The maximum PSi concentration in the pore water was 0.40 mmol L^{-1} at a

286   depth of 5 cm in September 2017 and it accounted for approximately 33% of the TSi.

287   The highest concentration of dissolved silicate was reported for ground water (1.0

288   mmol L^{-1}; Krauskopf and Bird 1995) and it has been suggested that dissolved silicate

289   exists in a polymeric form because, at this concentration, it is close to the monomeric

290   silicate solubility (1.4 mmol L^{-1}).

291   Van der Weijden (2007) stated that this highly concentrated dissolved silicate, eluted

292   from the lake sediments, likely originated from biomaterials such as diatom debris.

293   However, Lehtimäki et al. (2016) reported that the silicates eluted from sediments in an

294   anoxic-reducing freshwater lake were derived from inorganic oxides such as metal

295   oxides, and not biogenic silica.

296

297   **Adsorption of dissolved silicate onto ferric hydroxide precipitate and its**

298   **polymerization**

299   Figure 10 shows the changes in the adsorption ratio of silicate onto $Fe(OH)_3$ over 120

300   days. In this experiment, the fractions of PSi and MSi in the $Fe(OH)_3$ precipitate were

301   determined after the dissolution of the $Fe(OH)_3$ precipitate in a 0.02 mol L^{-1} HNO_3

302   solution, as described in the method section. The sum of TSi (PSi and MSi)

303   concentrations in the filtrate and the precipitate coincided with the initial concentration

304   of silicate detected at the beginning of the experiment. Only MSi was identified in the

305   filtrate, while PSi was not detected during the entire experimental period.

13

306   The adsorption ratio of silicate continuously increased over time. The adsorption

307   ratio was 45% on day 0, and then increased to 68% over the following 120 days. The

308   concentration of MSi in the precipitate was 0.32 mmol L^{-1} on day 0 and had decreased

309   to 0.21 mmol L^{-1} by the 40th day. On the 120th day, MSi in the precipitate had decreased

310   to 0.20 mmol L^{-1}. By contrast, the PSi concentration showed a value close to 0.00 mmol

311   L^{-1} on the initial day but increased to 0.21 mmol L^{-1} on the 40th day and 0.29 mmol L^{-1}

312   on the 120th day. The ratio of PSi to TSi concentrations in the precipitate increased from

313   0% on day 0 to 50% on the 40th day and 60% on the 120th day (Fig. 10). These results

314   show that silicates were transferred from the aqueous solution to the precipitate via

315   adsorption in the solution. After adsorption, MSi on Fe(OH)$_3$ was polymerized to PSi.

316   It is noteworthy that PSi was only detected in the precipitate and that the initial MSi

317   in the mixed solution was 0.7 mmol L^{-1}, which was less than half of the solubility of

318   MSi. Therefore, the adsorption of dissolved silicates is inferred as an essential process

319   for the polymerization of silicates.

320

321   **Stability of PSi**

322   The annual change in the distribution profile of PSi and TSi in Lake Biwa (Fig. 9)

323   shows that TSi concentrations were lower than 1.4 mmol L^{-1}, but PSi concentrations

324   were stable in the lake bottom throughout the anoxic-reducing period. Thus, it was not

325   clear how the PSi could dissolve in the pore water for an extended period under such

326   conditions.

327   Figure 11 presents the stability of PSi eluted from Fe(OH)$_3$ precipitates in different

328   conditions. A decrease in PSi concentration was observed only in aerobic conditions,

329   namely the HNO$_3$ + Aeration and Na$_2$S + Aeration conditions. Furthermore, PSi

14

330　concentration under HNO_3 + Aeration was rapidly depleted, only two days after

331　aeration. With Na_2S + Aeration, PSi concentration decreased from 0.44 mmol L^{-1} on the

332　1st day to 0.34 mmol L^{-1} on the 3rd day (Fig. 11), when H_2S + HS^- decreased to 0 mmol

333　L^{-1} (Fig. 12).

334　　On the other hand, in anaerobic conditions (anoxic-reducing conditions, HNO_3/Na_2S

335　+ Anaeration), the initial PSi concentration was maintained for 14 days of the

336　experiment, regardless of the chemical composition of the solution. Therefore, these

337　results suggest that PSi is stabilized under anaerobic conditions. In other words, PSi is

338　generally only observed in anaerobic water. Unfortunately, the precise mechanism by

339　which PSi is stabilized under anaerobic conditions is unknown at present. We will study

340　this mechanism in detail in the future.

341

342

343　**Conclusion**

344　　Polymerization of dissolved silicate was found to occur after its adsorption onto

345　$Fe(OH)_3$ in an oxidative environment, even if the TSi concentration was lower than 1.4

346　mmol L^{-1}, the solubility of monomeric silicate. The PSi was only detected in the pore

347　water of freshwater lakes where H_2S was generated in anoxic-reducing conditions.

348　When H_2S reacts with $Fe(OH)_3$ to form FeS, MSi and PSi in the hydroxide are released

349　into the pore water. Moreover, this PSi dissolves steadily in an anoxic-reducing

350　environment.

351

358

359 **References**

360 Aston S (1983) Natural water and atmospheric chemistry of silicon. In: Aston S (ed)

361   Silicon geochemistry and biogeochemistry. Academic Press, Massachusetts, US. pp

362   77-100

363 Conley D, Schelske C, Stoermer E (1993) Modification of the biogeochemical cycle of

364   silica with eutrophication. Mar Ecol Prog Ser 101: 179-192. DOI:

365   10.3354/meps101179

366 Cornelis JT, Delvaux B, Georg RB, Lucas Y, Ranger J, Opfergelt S (2011) Tracing the

367   origin of dissolved silicon transferred from various soil-plant systems towards rivers:

368   a review. Biogeosciences 8: 89-112. DOI: 10.5194/bg-8-89-2011

369 Fischer WW, Knoll AH (2009) An iron shuttle for deepwater silica in Late Archean and

370   early Paleoproterozoic iron formation. Geol Soc Am Bull 121: 222-235. DOI:

371   10.1130/B26328.1

372 Fukusawa H, Koizumi I, Okamura M, Yasuda Y (1995) Last 2,000 year records of

373   eolian dust concentration sea-level and precipitation changes in fine-grained sediment

374   of Lake Suigetsu, Central Japan (in Japanese). Chigaku Zasshi 104: 69-81. DOI:

375   10.5026/jgeography.104.69

376 Furumai H (2012) Monitoring of silicic acid and research implication (in Japanese). In:

377   Furumai H, Sato K, Yamamoto K (eds) Silicic acid, its source and transportation (in

378   Japanese). Gihodo Shuppan, Tokyo, Japan. pp 165-176

379 George S, Steinberg SM, Hodge V (2000) The concentration, apparent molecular weight

380   and chemical reactivity of silica from groundwater in Southern Nevada.

381   Chemosphere 40: 57-63. DOI: 10.1016/s0045-6535(99)00240-4

382 Hansen HP, Koroleff F (1999) Determination of nutrients. In: Grasshoff K, Kremling K,

383   Ehrhardt M (eds) Methods of seawater analysis. 3rd ed. Wiley, pp 159-228

384   Isshiki K, Sohrin Y, Nakayama E (1991) Form of dissolved silicon in seawater. Mar

385   Chem 32: 1-8. DOI: 10.1016/0304-4203(91)90021-N

386   Kawashima M, Hori T, Koyama M, Takamatsu T (1985) Redox cycle of manganese and

387   iron and the circulation of phosphorus in a dredged area of the Southern lake. In:

388   Takamatsu T (ed), Limnological and environmental studies of elements in the

389   sediment of Lake Biwa. The National Institute for Environmental Studies, Japan, pp

390   47-62

391   Krauskopf K, Bird D (1995) Sedimentation and Diagenesis: Inorganic Geochemistry.

392   In: Krauskopf K, Bird D (eds) Introduction to Geochemistry 3rd ed. McGraw-Hill,

393   New York, US. pp 356-384

394   Kusunoki K, Sakata M (2018) Analysis of historical trend of eutrophication in Lake

395   Nakaumi, Japan, using concentrations of several index elements in sediment cores (in

396   Japanese). Mizu Kankyo Gakkaishi 41:151-157. DOI: 10.2965/jswe.41.151

397   Kyotani T, Koshimizu S, Kobayashi H (2005) Short-term cycle of eolian dust (Kosa)

398   recorded in Lake Kawaguchi sediments, central Japan. Atmos Environ 39: 3335-

399   3342. DOI: 10.1016/j.atmosenv.2005.01.026

400   Lacombe M, Garçon V, Comtat M, Oriol L, Sudre J, Thouron D, Le Bris N, Provost C

401   (2007) Silicate determination in sea water Toward a reagentless electrochemical

402   method. Mar Chem 106: 489-497. DOI: 10.1016/j.marchem.2007.05.002

403   Lehtimäki M, Sinkko H, Tallberg P (2016) The role of oxygen conditions in the

404   microbial dissolution of biogenic silica under brackish conditions. Biogeochemistry

405   129: 355-371. DOI: 10.1007/s10533-016-0237

406   Lehtoranta J, Ekholm P, Pitkänen H (2009) Coastal eutrophication thresholds: a matter

407   of sediment microbial processes. Ambio 38: 303-308. DOI: 10.1579/09-A-656.1

408   Li X, Song J, Dai J, Yuan H, Li N, Li F, Sun S (2006) Biogenic silicate accumulation in

409   sediments, Jiaozhou Bay. Chin J Oceanol Limnol 24: 270-077. DOI:

410   10.1007/BF02842627

411   Maekawa K, Shirasaki K, Sawada T, Yamaguchi S, Utsunomiya T, Aoki K, Tagawa S,

412   Isomatsu Y (1982) Study on the eutrophication of Lakes Mikata Goko: Horizontal

413   distribution of water quality of the lakes (in Japanese). Annual Report of The

414   Environmental Pollution Research Center of Fukui Prefecture, Japan, pp 181-185

415   Nagasaka M, Yoshizawa K, Ariizumi K, Hirabayashi K (2002) Temporal changes and

416   vertical distribution of macrophytes in Lake Kawaguchi. Limnology 3: 107-114.

417   DOI: 10.1007/s102010200012

418   Nalewajko C, Murphy T (2001) Effects of temperature, and availability of nitrogen and

419   phosphorus on the abundance of Anabaena and Microcystis in Lake Biwa, Japan: an

420   experimental approach. Limnology 2: 45-48. DOI: 10.1007/s102010170015

421   Ning R (2002) Discussion of silica speciation, fouling, control and maximum reduction,

422   Desalination 151: 67-73. DOI: 10.1016/S0011-9164(02)00973-6

423   O'Connor T (1961) The reaction rates of polysilicic acids with molybdic acid. J Phys

424   Chem 65: 1-5. DOI: 10.1021/j100819a001

425   Park JY, Sugahara S, Egawa M, Seike Y (2020) Mechanism of silicate elution by

426   hydrogen sulfide from bottom sediment in a brackish lake. Limnology 21: 197-205.

427   DOI: 10.1007/s10201-019-00601-2

428   Park JY, Sugiyama M (2018) Formation and decomposition of polymeric silicate in pore

429   water, 17th World Lake Conference proceedings, Lake Kasumigaura, Ibaraki, Japan,

430   pp 1159-1161

431   Perry C, Keeling-Tucker T (2000) Biosilicification: the role of the organic matrix in

432   structure control. J Biol Inorg Chem 5: 537-550. DOI: 10.1007/s007750000130

433   Pollingher U (1990) Effects of latitude on phytoplankton composition and abundance in

434   large lakes. In: Tilzer M, Serruya C (eds) Large lakes: Ecological structure and

435   function. Springer, Berlin, Germany. pp 368-402

436   Schelske C, Stoermer E (1971) Eutrophication, silica depletion, and predicted changes

437   in algal quality in Lake Michigan. Science 173: 423-424. DOI:

438   10.1126/science.173.3995.423

439   Sjöberg S (1996) Silica in aqueous environment. J Non-Cryst Solids 196: 51-57. DOI:

440   10.1016/0022-3093(95)00562-5

441   Sugahara S, Yurimoto T, Ayukawa K, Kimoto K, Senga Y, Okumura M, Seike Y (2010)

442   A simple in situ extraction method for dissolved sulfide in sandy mud sediments

443   followed by spectrophotometric determination and its application to the bottom

444   sediment at the Northeast of Ariake Bay (in Japanese). Bunseki Kagaku 59: 1155-

445   1161. DOI: 10.2116/bunsekikagaku.59.1155

446   Swedlund PJ, Webster JG (1999) Adsorption and polymerisation of silicic acid on

447   ferrihydrite, and its effect on arsenic adsorption. Water Research 33: 3413-3422. DOI:

448   10.1016/S0043-1354(99)00055-X

449   Tallberg P (2000) Silicon and its impacts on phosphorus in eutrophic freshwater lakes.

450   Ph. D. thesis. Univ of Helsinki

451   Tanaka M (1992) The Lakes in Japan (in Japanese). Nagoya University, Japan

452   Tanaka M, Takahashi K, Nemoto M, Horimoto N (2013) Selectivity of silica species in

453   ocean observed from seasonal and local changes. Spectrochim Acta, Part A 104: 423-

454   427. DOI: 10.1016/j.saa.2012.11.040

455   Tarutani T (1989) Polymerization of silicic acid a review. Anal Sci 5: 245-252. DOI:

456   10.2116/analsci.5.245

457   Terashima A, Ueda T (1982) Effect of bottom dredging on some environmental factors

458   and benthic animals in the South basin of Lake Biwa (in Japanese). Jpn J Limnol 43:

459   81-87. DOI: 10.3739/rikusui.43.81

460   Tréguer P, Nelson D, Van Bennekom A, de Master D, Leynaert A, Quéguiner B (1995)

461   The silica balance in the world ocean: a reestimate. Science 268: 375-379. DOI:

462   10.1126/science.268.5209.375

463   Valdes LM, Price KS, Luther III GW (2002) Iron sulfur phosphorus cycling in the

464   sediments of a shallow coastal bay: implications for sediment nutrient release and

465   benthic macroalgal blooms. Limnol Oceanogr 47: 1346-1354. DOI:

466   10.4319/lo.2002.47.5.1346

467   Van der Weijden C (2007) Silica I: silicon analytical, physical and terrestrial

468   geochemistry, Ph. D. thesis. Utrecht University

469   Wang D (2008) Neurotoxins from marine dinoflagellates: a brief review. Mar Drugs 6:

470   349-371. DOI: 10.3390/md20080016

471   Willén E (1991) Planktonic diatoms - an ecological review. Archiv für Hydrobiologie.

472   Supplementband, Algological studies 62: 69-106. ISSN 0342-1120

473   Yamamoto S, Nakamura T, Uchiyama T (2017) Newly discovered lake bottom springs

474   from Lake Kawaguchi, the Northern foot of Mount Fuji, Japan, Journal of Japanese

475   Association of Hydrological Sciences 47: 49-59. DOI: 10.4145/jahs.47.49

476   Yee N, Phoenix V, Konhauser K, Benning L, Ferris G (2003) The effect of

477   cyanobacteria on silica precipitation at neutral pH: implications for bacterial

478   silicification in geothermal hot springs. Chem Geol 199: 83-90. DOI: 10.1016/S0009-

479   2541(03)00120-7

480   Zuhl RW, Amjad Z (2013) Solution chemistry impact on silica polymerization by

481   inhibitors. In: Amjad Z (ed) Mineral Scales in Biological and Industrial Systems.

482   CRC Press, Florida, US. pp 173-200

Figure legends

Figure 1 Sampling points in each lake (Lake Nakaumi, 35.43°N 144.27°E; Lake Suigetsu,

35.58°N 135.88°E; Lake Suga, 35.58°N 135.90°E; Lake Biwa, 35.00°N 135.57°E; Lake

Kawaguchi, 35.51°N 138.73°E).

Figure 2 Schematic experimental process to evaluate PSi stability. The 0.4-μm nuc

leopore filter was used to separate the silicates adsorbed on $Fe(OH)_3$ precipitate f

rom the initial solution (the mixture of MSi and DFe). Moreover, the 0.2-μm nu

cleopore filter was used to remove FeS precipitate, including the colloidal FeS c

ompletely.

Figure 3 Vertical profiles of TSi (□), MSi (○), and PSi (▲) in the pore water of Lake

Nakaumi (August 21, 2017). No significant difference was observed between TSi and

MSi concentrations.

Figure 4 Vertical profiles of TSi (□), MSi (○), and PSi (▲) in the pore waters of Lakes

Suigetsu (left) and Suga (right) on May 20, 2017.

Figure 5 Vertical profiles of DO in Lake Biwa (●, September 21, 2017) and Lake

Kawaguchi (○, September 30, 2017).

Figure 6 Vertical profiles of DFe and $H_2S + HS^-$ in the pore waters of Lake Biwa (●,

September 21, 2017) and Lake Kawaguchi (○, September 30, 2017).

Figure 7 Vertical profiles of TSi (□), MSi (○), and PSi (▲) in the pore waters of Lake

Biwa (left; September 21, 2017) and Lake Kawaguchi (right; September 30, 2017).

503   Figure 8 Annual change in DO concentration in the hypolimnion layer (water depth: 12

504   m) of Lake Biwa.

505   Figure 9 Vertical profiles of DFe ($\blacksquare$), H_2S +HS^- ($\triangle$), TSi ($\square$), MSi ($\bigcirc$), and PSi ($\blacktriangle$)

506   in the pore water of Lake Biwa from March 14 to December 15, 2017.

507   Figure 10 Formation of polymeric silicate in the adsorption reaction of silicate onto

508   ferric hydroxide, over 120 days. Only the concentrations of TSi ($\square$), MSi ($\bigcirc$), and PSi

509   ($\blacktriangle$) in the precipitate are presented.

510   Figure 11 Stability of PSi under each set of conditions, namely HNO_3 + Aeration ($\bigcirc$),

511   HNO_3 + Anaeration ($\square$), Na_2S + Aeration ($\bullet$), and Na_2S + Anaeration ($\blacktriangle$), over 14

512   days.

513   Figure 12 Changes in the concentration of H_2S + HS^- and DO under each set of

514   conditions, over two weeks. $\square$: DO in HNO_3 + Aeration, $\bullet$: DO in Na_2S + Aeration,

515    $\triangle$: H_2S + HS^- in Na_2S + Aeration, and $\blacktriangle$: H_2S + HS^- in Na_2S + Anaeration. Note that

516   concentrations of DO in HNO_3 + Anaeration, DO in Na_2S + Anaeration, and H_2S + HS^-

517   in HNO_3 + Aeration/Anaeration have been omitted because these values were 0 mg-O_2

518   L^{-1} (DO) or 0 mmol L^{-1} (H_2S + HS^-) throughout the experimental period.

519

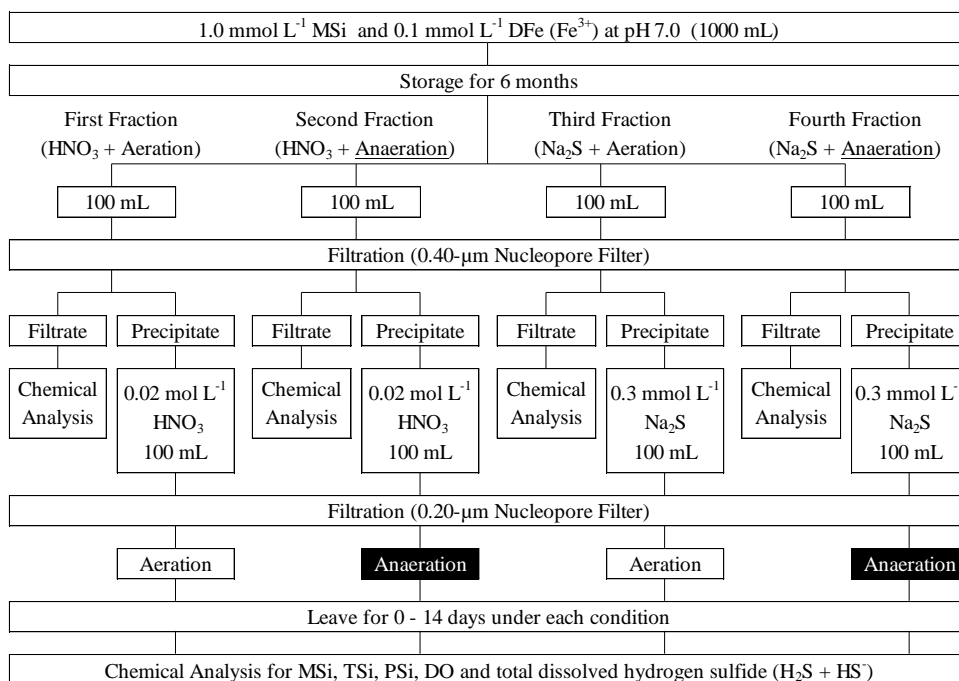520
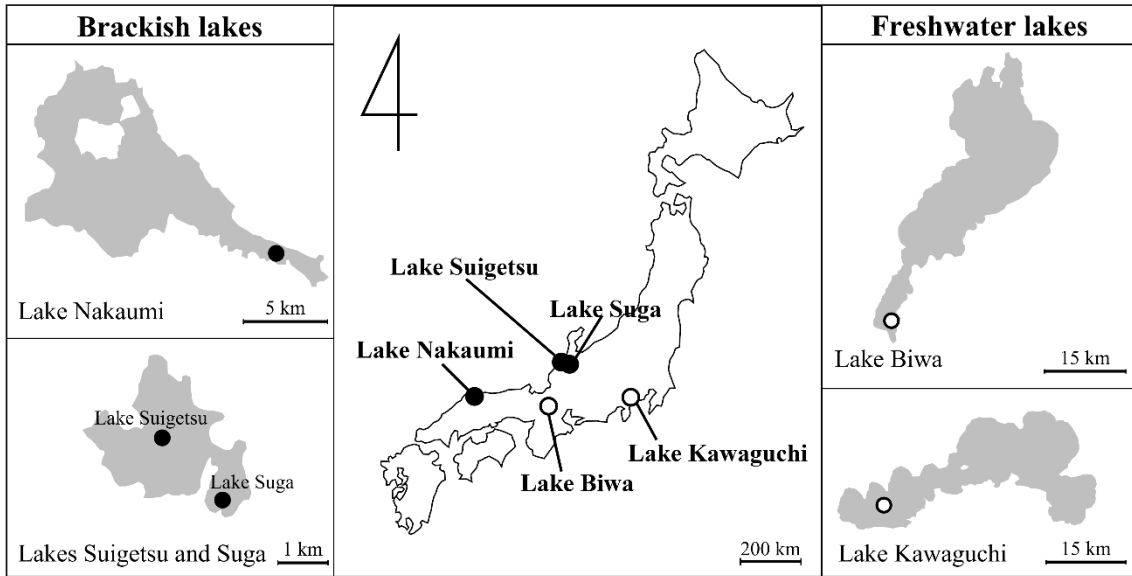
Figures

Figure 1 Sampling points in each lake (Lake Nakaumi, 35.43°N 144.27°E; Lake Suigets u, 35.58°N 135.88°E; Lake Suga, 35.58°N 135.90°E; Lake Biwa, 35.00°N 135.57°E; La ke Kawaguchi, 35.51°N 138.73°E).
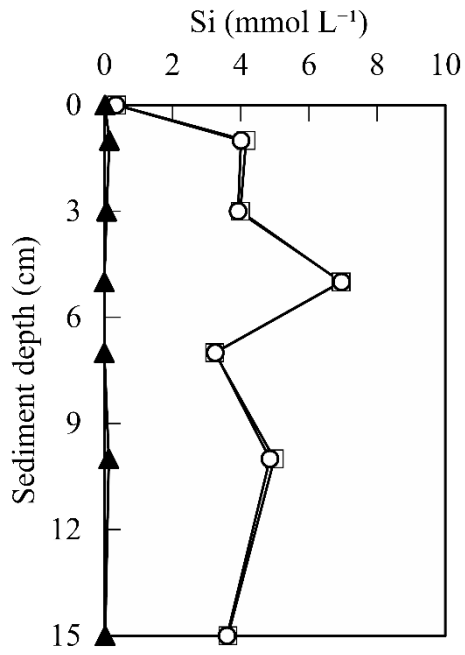
```
┌─────────────────────────────────────────────────────────────────────────────────┐
│          1.0 mmol L⁻¹ MSi  and 0.1 mmol L⁻¹ DFe (Fe³⁺) at pH 7.0  (1000 mL)        │
└─────────────────────────────────────────────────────────────────────────────────┘
┌─────────────────────────────────────────────────────────────────────────────────┐
│                              Storage for 6 months                                 │
└─────────────────────────────────────────────────────────────────────────────────┘

   First Fraction          Second Fraction          Third Fraction          Fourth Fraction
 (HNO₃ + Aeration)       (HNO₃ + Anaeration)       (Na₂S + Aeration)       (Na₂S + Anaeration)

    ┌─────────┐            ┌─────────┐             ┌─────────┐             ┌─────────┐
    │ 100 mL  │            │ 100 mL  │             │ 100 mL  │             │ 100 mL  │
    └─────────┘            └─────────┘             └─────────┘             └─────────┘

┌─────────────────────────────────────────────────────────────────────────────────┐
│                    Filtration (0.40-µm Nucleopore Filter)                         │
└─────────────────────────────────────────────────────────────────────────────────┘

 ┌────────┬─────────┐   ┌────────┬─────────┐   ┌────────┬─────────┐   ┌────────┬─────────┐
 │Filtrate│Precipitate│ │Filtrate│Precipitate│ │Filtrate│Precipitate│ │Filtrate│Precipitate│
 ├────────┼─────────┤   ├────────┼─────────┤   ├────────┼─────────┤   ├────────┼─────────┤
 │Chemical│0.02 mol L⁻¹│ │Chemical│0.02 mol L⁻¹│ │Chemical│0.3 mmol L⁻¹│ │Chemical│0.3 mmol L⁻¹│
 │Analysis│  HNO₃   │   │Analysis│  HNO₃   │   │Analysis│  Na₂S   │   │Analysis│  Na₂S   │
 │        │ 100 mL  │   │        │ 100 mL  │   │        │ 100 mL  │   │        │ 100 mL  │
 └────────┴─────────┘   └────────┴─────────┘   └────────┴─────────┘   └────────┴─────────┘

┌─────────────────────────────────────────────────────────────────────────────────┐
│                    Filtration (0.20-µm Nucleopore Filter)                         │
└─────────────────────────────────────────────────────────────────────────────────┘

    ┌─────────┐            ┌─────────────┐         ┌─────────┐            ┌─────────────┐
    │ Aeration│            │█Anaeration█ │         │ Aeration│            │█Anaeration█ │
    └─────────┘            └─────────────┘         └─────────┘            └─────────────┘

┌─────────────────────────────────────────────────────────────────────────────────┐
│                     Leave for 0 - 14 days under each condition                     │
└─────────────────────────────────────────────────────────────────────────────────┘
┌─────────────────────────────────────────────────────────────────────────────────┐
│   Chemical Analysis for MSi, TSi, PSi, DO and total dissolved hydrogen sulfide (H₂S + HS⁻)  │
└─────────────────────────────────────────────────────────────────────────────────┘
```

Figure 2 Schematic experimental process to evaluate PSi stability. The 0.4-µm

nucleopore filter was used to separate the silicates adsorbed on $Fe(OH)_3$ precipitate

from the initial solution (the mixture of MSi and DFe). Moreover, the 0.2-µm

nucleopore filter was used to remove FeS precipitate, including the colloidal FeS
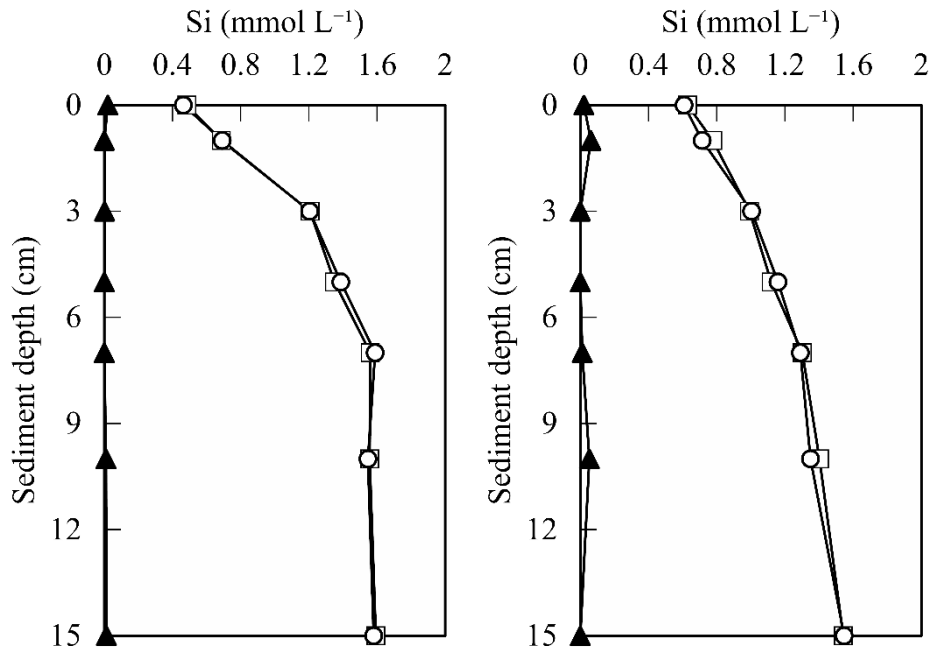
completely.

534

535   Figure 3 Vertical profiles of TSi (□), MSi (○), and PSi (▲) in the pore water of Lake

536   Nakaumi (August 21, 2017). No significant difference was observed between TSi and
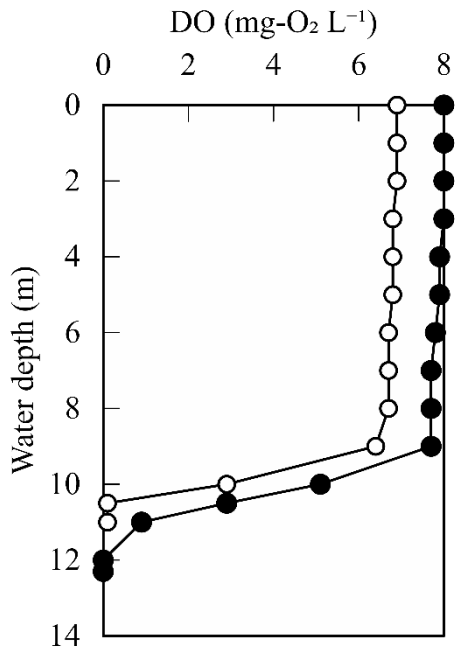
537   MSi concentrations.

538

539

540

27

541

542   Figure 4 Vertical profiles of TSi (□), MSi (○), and PSi (▲) in the pore waters of Lakes

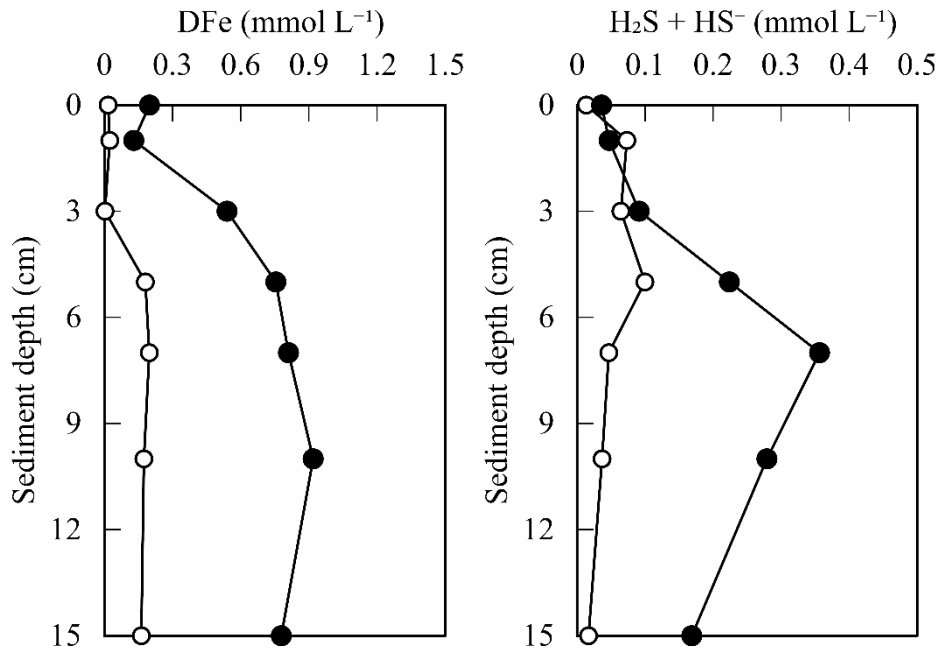543   Suigetsu (left) and Suga (right) on May 20, 2017.

544

545

546

547   Figure 5 Vertical profiles of DO in Lake Biwa (●, September 21, 2017) and Lake

548   Kawaguchi (○, September 30, 2017).

549

550

551   Figure 6 Vertical profiles of DFe and H_2S + HS^- in the pore waters of Lake Biwa (●,

552   September 21, 2017) and Lake Kawaguchi (○, September 30, 2017).

553

554
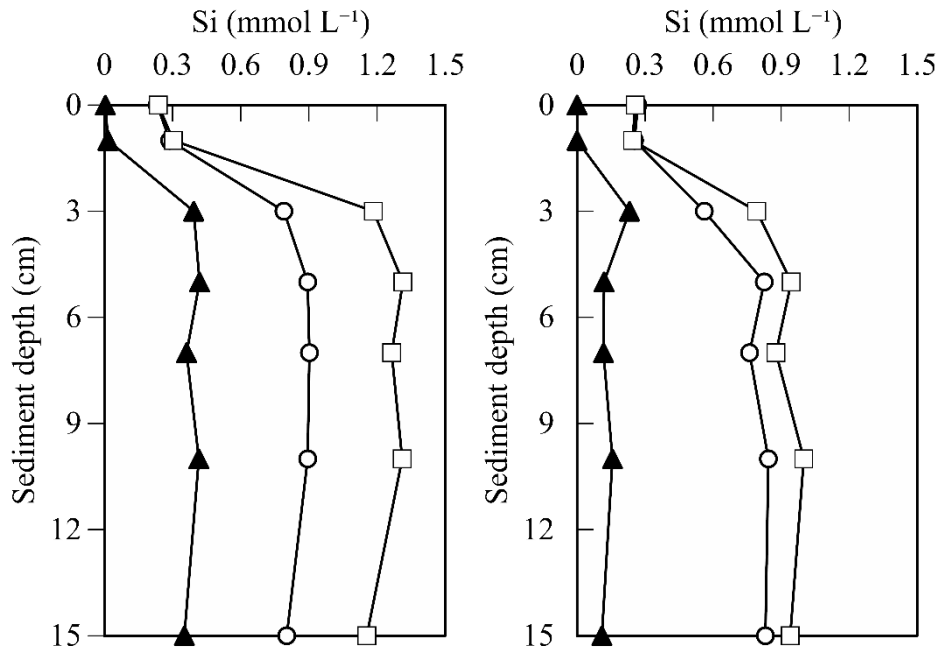
Figure 7 Vertical profiles of TSi (□), MSi (○), and PSi (▲) in the pore waters of Lake

556   Biwa (left; September 21, 2017) and Lake Kawaguchi (right; September 30, 2017).

557

558

559

31
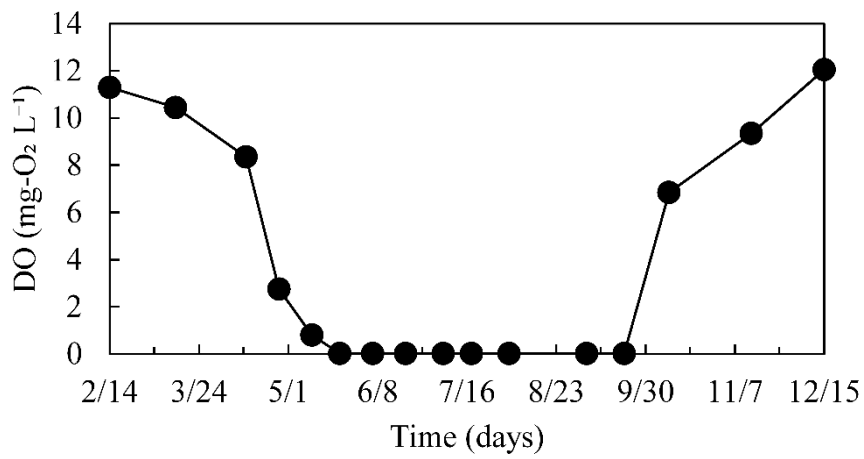
560

561   Figure 8 Annual change in DO concentration in the hypolimnion layer (water depth: 12
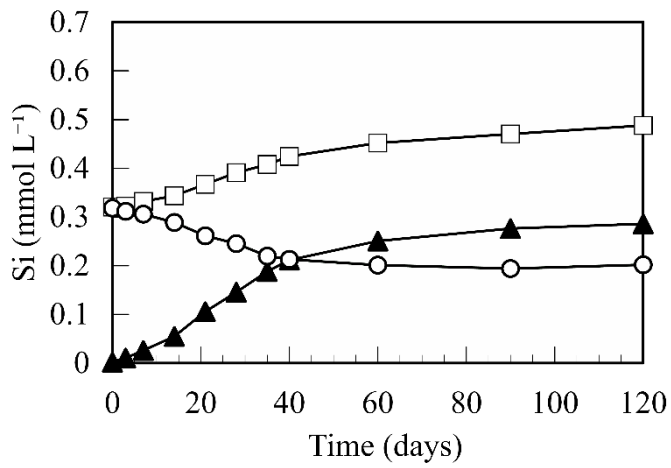
562   m) of Lake Biwa.

563

564
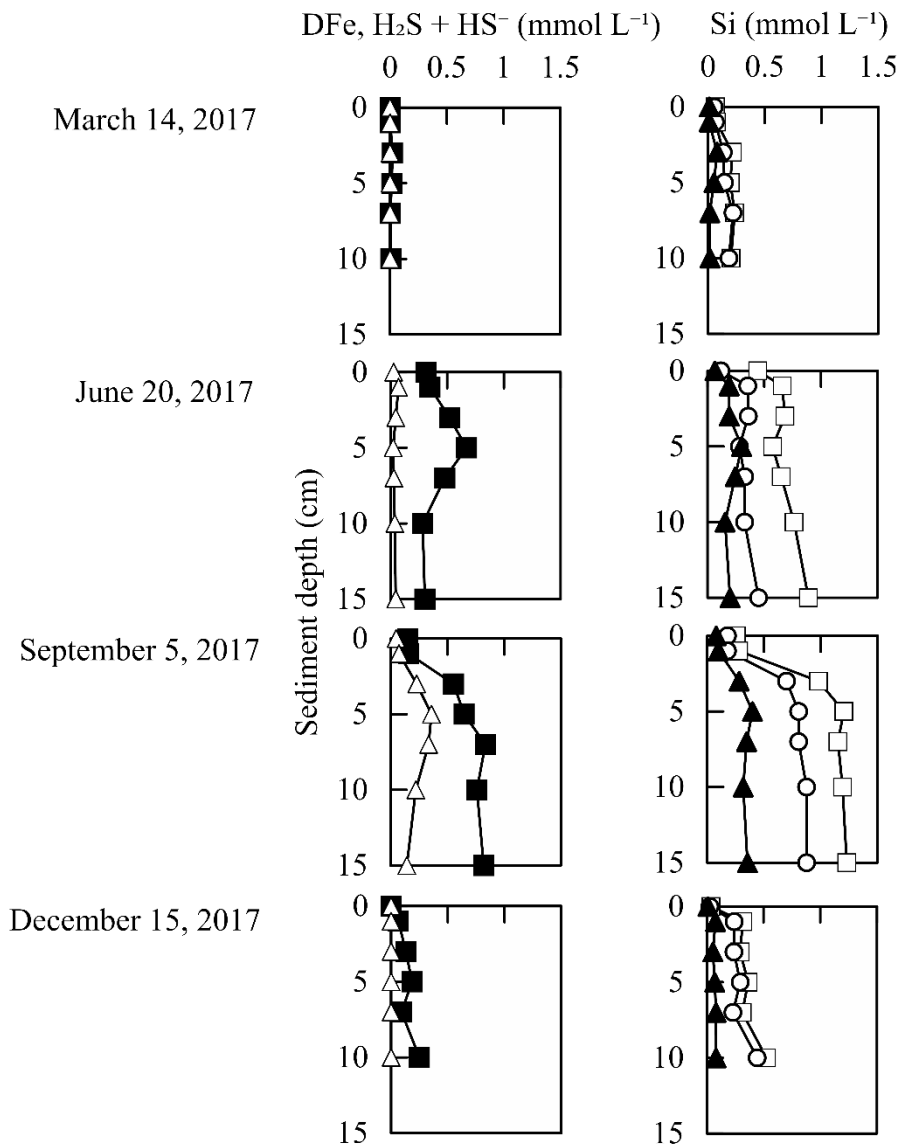
DFe, H₂S + HS⁻ (mmol L⁻¹)   Si (mmol L⁻¹)

565

Figure 9 Vertical profiles of DFe (■), H₂S +HS⁻ (△), TSi (□), MSi (○), and PSi (▲)

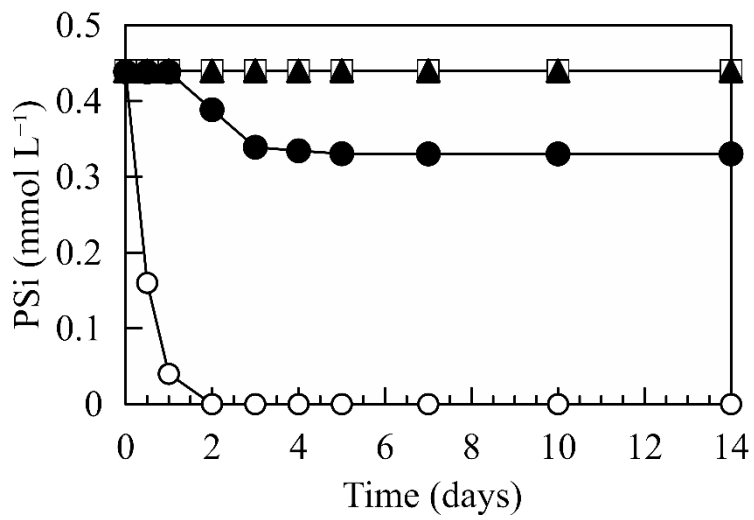in the pore water of Lake Biwa from March 14 to December 15, 2017.

568

569

570 Figure 10 Formation of polymeric silicate in the adsorption reaction of silicate onto

571 ferric hydroxide, over 120 days. Only the concentrations of TSi ($\square$), MSi ($\bigcirc$), and PSi

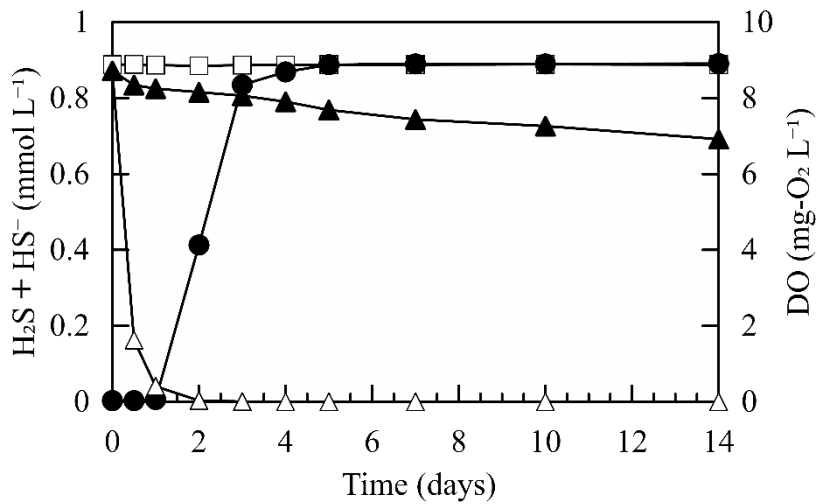572 ($\blacktriangle$) in the precipitate are presented.

573

574

575

576

577   Figure 11 Stability of PSi under each set of conditions, namely HNO_3 + Aeration (○),

578   HNO_3 + Anaeration (□), Na_2S + Aeration (●), and Na_2S + Anaeration (▲), over 14

579   days.

580

581

582 Figure 12 Changes in the concentration of $H_2S + HS^-$ and DO under each set of

583 conditions, over two weeks. □: DO in HNO_3 + Aeration, ●: DO in Na_2S + Aeration,

584 △: $H_2S + HS^-$ in Na_2S + Aeration, and ▲: $H_2S + HS^-$ in Na_2S + Anaeration. Note that

585 concentrations of DO in HNO_3 + Anaeration, DO in Na_2S + Anaeration, and $H_2S + HS^-$

586 in HNO_3 + Aeration/Anaeration have been omitted because these values were 0 mg-O_2

587 L^{-1} (DO) or 0 mmol L^{-1} ($H_2S + HS^-$) throughout the experimental period.

588